A Generic Synthetic Approach to Large-Scale Pristine-Graphene/Metal-Nanoparticles Hybrids

Xiujuan Wang, Guowen Meng, Chuhong Zhu, Zhulin Huang, Yiwu Qian, Kexi Sun, and Xiaoguang Zhu*

The homogeneous attachment of metal-nanoparticles (metal-NPs) on pristine-graphene surface to construct pristine-graphene/metal-NPs hybrids is highly expected for application in many fields such as transparent electrodes and conductive composites. However, it remains a great challenge since the pristine-graphene is highly hydrophobic. Here, an environmentally friendly generic synthetic approach to large-scale pristine-graphene/metal-NPs hybrids is presented, by a combinatorial process of exfoliating expanded graphite in N-methyl pyrrolidone via sonication and centrifugation to achieve the pristine-graphene, and attaching pre-synthesized metal-NPs on the pristine-graphene in ethanol via van der Waals interactions between the metal-NPs and the pristine-graphene. Nanoparticles of different metals (such as Ag, Au, and Pd) with various morphologies (such as sphere, cube, plate, multi-angle, and spherical-particle assembling) can be homogeneously attached on the defect-free pristine-graphene with controlled packing densities. Both the pristine-graphene and the metal-NPs preserve their original intrinsic structures. The as-synthesized pristine-graphene/Ag-NPs hybrids show very high surface-enhanced Raman scattering activity due to the combined effects of large surface area of the pristine-graphene to adsorb more target molecules and the electromagnetic enhancement of the Ag-NPs. This large-scale synthesis of the pristine-graphene/metal-NPs hybrids with tunable shape and packing density of metal-NPs opens up opportunities for fundamental research and potential applications ranging from devices to transparent electrodes and conductive composites.

1. Introduction

Graphene, a two-dimensional lattice of carbon with a thickness of only a single atom's diameter, has attracted attention due to its outstanding electronic, mechanical, and chemical properties.[1–4] These unique properties make graphene a promising building block in the hybridization with various materials.[5–13] To date, graphene-based hybrids have become a hot research topic because the hybridization can enable versatile and tunable properties with performances far beyond those of the individual counterpart materials, and the integration of nanomaterials on graphene paves a new way to enhance their electronic, optical, mechanical, and electrochemical properties.[14–20] Especially, the fabrication of graphene/metal-nanoparticles (NPs) hybrids is of significant interest due to their potential applications in catalysis, chemical sensing, surface-enhanced Raman scattering (SERS), and battery electrodes.[21–30]

To date, much progress has been made to the fabrication of the graphene/metal-NPs hybrids, such as graphene/Ag-NPs,[21,22] graphene/Au-NPs,[23,24] graphene/Pd-NPs,[25,26] and graphene/Pt-NPs[27,28] hybrids. However, the homogeneous attachment of metal-NPs on pristine-graphene (without oxidation or any other treatment) to construct pristine-graphene/metal-NPs hybrids is still a challenge since the pristine-graphene is highly hydrophobic.[31] Among the most reported approaches for the fabrication of the graphene/metal-NPs hybrids, graphene oxide (GO) and reduced-GO (RGO), which can be considered as chemically functionalized graphene with hydroxyls and epoxides, are usually used as 2D matrix to attach metal-NPs.[32] Up to now, a large number of GO(RGO)/metal-NPs systems have been fabricated.[21–28,33–37] Although these GO(RGO)/metal-NPs hybrids have been demonstrated to display enhanced performance in many fields including catalysis,[25,26] SERS,[21,22] and electrochemical sensor,[27,28] they suffer from some intrinsic limitations such as poor conductivity induced by the large quantities of defects in GO or RGO that disrupt the band structure and completely degrade the electronic properties.[38–40] In fact, the GO is electrically insulating; although chemical reduction can partially recover its conductivity, the recovered conductivity is still below that of the pristine-graphene with orders of magnitude.[38] The poor conductivity of the GO (RGO)/metal-NPs hybrids severely restricts their promising applications in many fields such as conductive electrodes. Therefore, it is highly

Dr. X. Wang, Prof. G. Meng, Dr. C. Zhu,
Dr. Z. Huang, Dr. Y. Qian, Dr. K. Sun, Dr. X. Zhu
Key Laboratory of Materials Physics and Anhui Key Laboratory of Nanomaterials and Nanostructures
Institute of Solid State Physics
Chinese Academy of Sciences
Hefei, 230031, P. R. China
University of Science and Technology of China
Hefei, 230026, P. R. China
E-mail: gwmeng@issp.ac.cn

DOI: 10.1002/adfm.201301409

© 2013 WILEY-VCH Verlag GmbH & Co. KGaA, Weinheim

desirable to develop effective and generic methods to fabricate the pristine-graphene/metal-NPs hybrids.

Although the growth of Ag-NPs on the pristine-graphene was recently achieved by in-situ reduction of Ag-precursor on the pristine-graphene,[30] the in-situ reduction of metal-precursor has not realized homogeneous attachment of different metal-NPs on the pristine-graphene, and it will be also difficult to control the morphology of the metal-NPs attached on the pristine-graphene, which is very important to the practical applications such as catalysis and SERS. In addition, the organic molecules used in the in-situ reduction of metal-precursor may degrade the favorable properties of the pristine-graphene/metal-NPs hybrids, and thus, might restrict their practical applications.

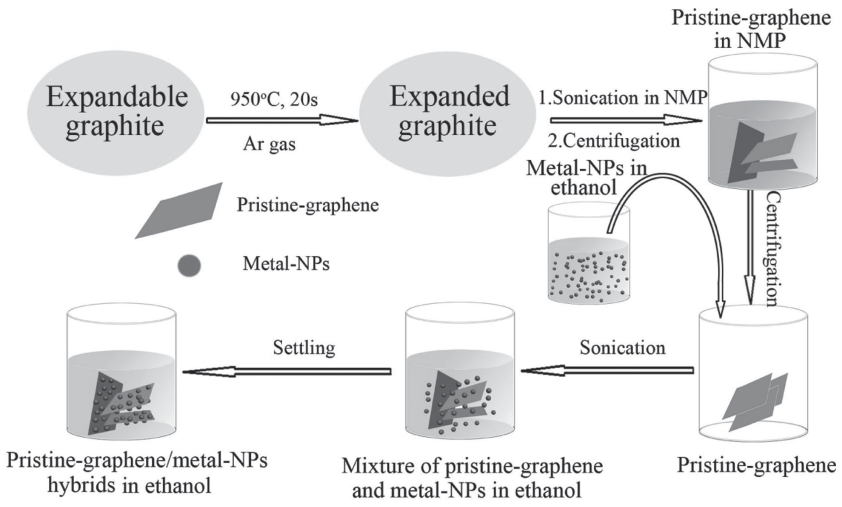

Scheme 1. Schematic illustration for the synthesis of the pristine-graphene/metal-NPs hybrids.

Herein, we present a simple, environmentally friendly, and generic synthetic approach to large-scale pristine-graphene/metal-NPs hybrids, by a combinatorial process of exfoliating expanded graphite in N-methyl pyrrolidone (NMP) via sonication and centrifugation to achieve pristine-graphene sheets, and attaching pre-synthesized metal-NPs on the pristine-graphene sheets in ethanol via van der Waals interactions between the metal-NPs and the pristine-graphene. Nanoparticles of different metals (such as Ag, Au, and Pd) with various morphologies (such as sphere, cube, plate, multi-angle, and spherical-particle assembling) have been homogeneously attached on the defect-free pristine-graphene surface with controlled packing densities. It is especially worth mentioning that no surface modification on the pristine-graphene or the metal-NPs is needed in the fabrication process of pristine-graphene/metal-NPs hybrids, thus avoiding the disruption of the intrinsic properties of the pristine-graphene and the metal-NPs by extra functional molecules and facilitating their practical applications. The as-synthesized pristine-graphene/Ag-NPs hybrids show high SERS activity due to the combined effects of large surface area of the pristine-graphene to adsorb more target molecules and the electromagnetic enhancement of Ag-NPs, and may serve as ultrasensitive SERS substrates for the rapid detection of chemical and biological analytes.

2. Results and Discussions

The strategy for the synthesis of the pristine-graphene/metal-NPs hybrids is shown in **Scheme 1**. Firstly, the pristine-graphene sheets were prepared by exfoliating expanded graphite in NMP solution[41,42] (details can be found in the Experimental Section). **Figure 1** are the transmission electron microscopy (TEM) images and the selected area electron diffraction (SAED) patterns of the as-prepared pristine-graphene sheets, with typical monolayer (Figure 1a,b), bilayer (Figure 1c,d), and multilayer (Figure 1e,f).[42] The monolayer pristine-graphene was in the folded structure, as shown in Figure 1a. The SAED pattern (Figure 1b) clearly shows the typical six-fold symmetry of the as-prepared pristine-graphene, which is similar to that of "peeled off" graphene,[43] inferring that the as-prepared pristine-graphene sheets have perfect crystalline structure. The high quality of the as-prepared pristine-graphene sheets has been further confirmed by Raman spectra (Figure S1a, Supporting Information). The spectra of bulk graphite were given for comparison. Two typical features of G peak at ≈1580 cm^{-1} and 2D peak at ≈2700 cm^{-1} for graphene/graphite can be clearly seen.[44,45] However, the D peak at ≈1350 cm^{-1}, which is considered as defect-induced Raman band, is nearly invisible in the spectra,[45] demonstrating the absence of significant structure defects in the as-prepared pristine-graphene. Furthermore, X-ray photoelectron spectroscopy (XPS) was performed to further illustrate the structural characteristics of the as-prepared pristine-graphene. The XPS spectra of bulk graphite were also given for comparison. As shown in the XPS survey spectra (Figure S1b, Supporting

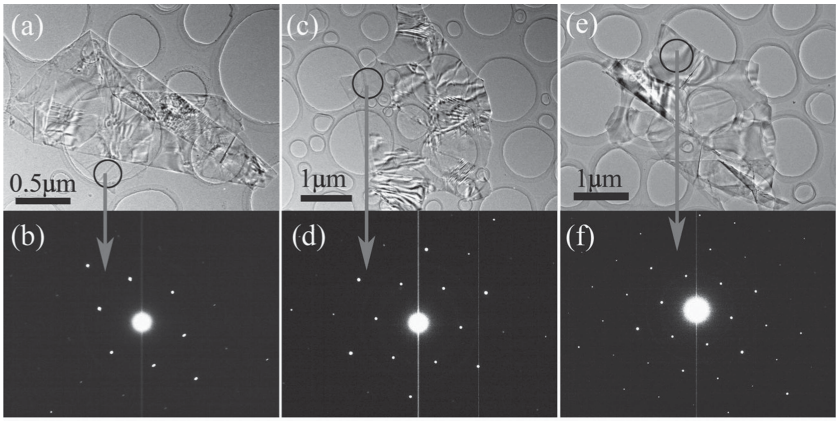

Figure 1. TEM images and SAED patterns of the as-synthesized pristine-graphene with a,b) monolayer, c,d) bilayer, and e,f) multilayer. The marked circles in the images indicate where the corresponding SAED pattern is taken.

© 2013 WILEY-VCH Verlag GmbH & Co. KGaA, Weinheim

Information), a weak O peak can be observed except for the C peak, indicating that there exist small amounts of O atoms on the pristine-graphene. The high resolution O1s XPS spectra (Figure S1c, Supporting Information) show the O peak located at 532.5 eV, being ascribed to the physisorbed hydrated O species.[46] The high resolution C1s XPS spectra (Figure S1d, Supporting Information) show only C–C bond with the banding energy of 284.6 eV, the absence of C–O bond (287.1 eV) and C=O bond (288.8 eV) further confirming the absence of defects in the form of oxides in the as-prepared pristine-graphene.[47]

Then the as-prepared pristine-graphene sheets were used as a 2D matrix for the attachment of metal-NPs. To achieve this purpose, the pristine-graphene dispersion in NMP was fast centrifuged, and then the aggregates of pristine-graphene were mixed with the pre-synthesized metal-NPs in ethanol by brief sonication. The resultant solution was centrifuged and then re-suspended in ethanol. After several hours of settling, almost all the metal-NPs were spontaneously absorbed on the surface of the pristine-graphene sheets. First, we tried Ag-NPs with spherical morphology. The photographs of the as-prepared pristine-graphene dispersed in NMP, the Ag-NPs in ethanol and the pristine-graphene/Ag-NPs hybrids in ethanol are shown in the Supporting Information, Figure S2a–c, respectively. The pristine-graphene/Ag-NPs hybrids form a stable suspension in ethanol, slow settling of the composite can be seen after several days, and mild sonication of the sample facilitates its re-suspension.

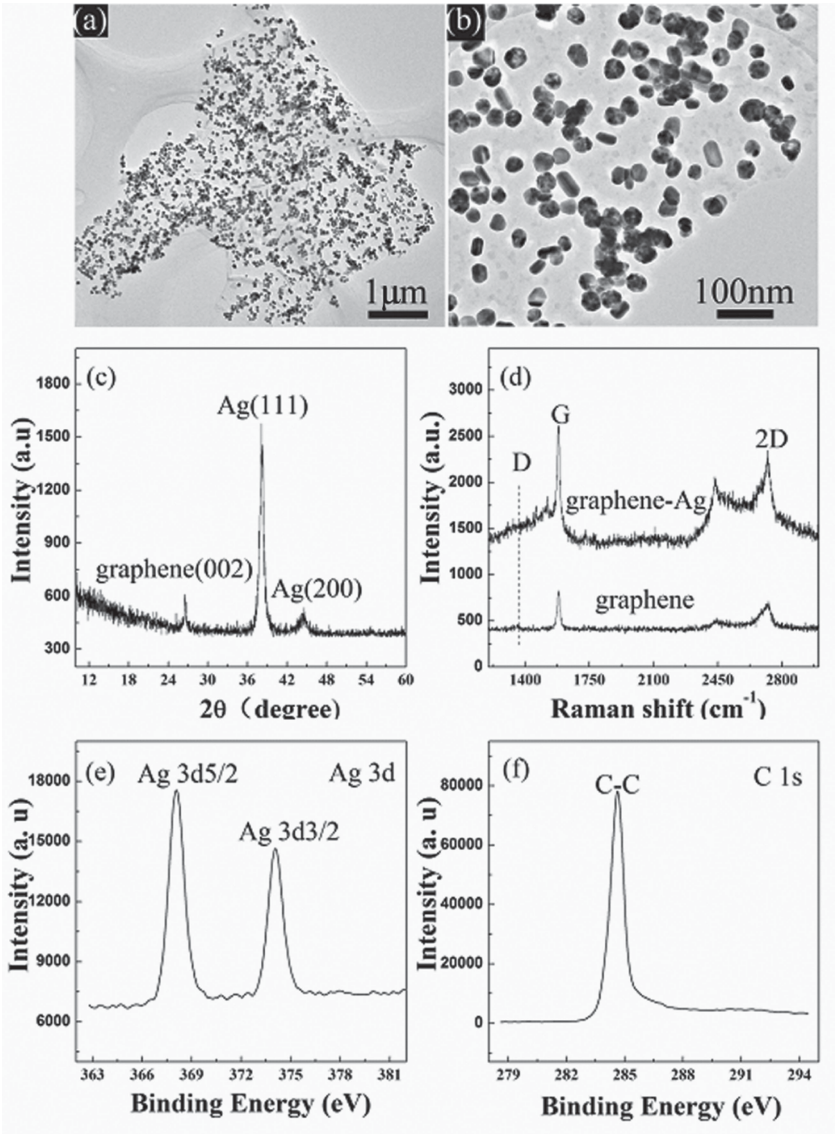

Figure 2. a,b) TEM images of the pristine-graphene/Ag-NPs hybrids at different magnifications. c) XRD pattern of the pristine-graphene/Ag-NPs hybrids. d) Raman spectra of the pristine-graphene and the pristine-graphene/Ag-NPs hybrids, respectively. e) XPS spectrum of Ag 3d in the pristine-graphene/Ag-NPs hybrids. f) XPS spectrum of C 1s in the pristine-graphene/Ag-NPs hybrids.

To reveal the distribution of the Ag-NPs on the pristine-graphene, the as-synthesized pristine-graphene/Ag-NPs hybrids were observed under TEM (**Figure 2**a,b). It can be seen clearly that the spherical Ag-NPs are uniformly distributed on the pristine-graphene sheets, and almost no particles scattered out of the supports, indicating the strong interaction between the Ag-NPs and the pristine-graphene sheets. It should be mentioned that the density of the Ag-NPs on the pristine-graphene surface could be easily controlled by tailoring the mass ratios of the pristine-graphene to the Ag-NPs mixed in ethanol (Figure S3, Supporting Information). Generally, the nanoparticles can be attached to the graphene via covalent or non-covalent interactions such as van der Waals interactions, π–π stacking, or electrostatic interactions.[48–52] In our case, the attachment process could not be attributed to covalent interaction as both the pristine-graphene and the Ag-NPs have not been modified with any functional groups. For the non-covalent interactions, π–π stacking is impossible as no aromatic organic molecules were modified on the Ag-NPs. Besides, electrostatic interaction is also impossible since the pristine-graphene do not carry any surface charges. Therefore, the attachment of Ag-NPs on the pristine-graphene surface is most likely due to the van der Waals interactions; this process is similar to the attachment of Au-NPs on carbon nanotubes by van der Waals interactions.[53] In addition, it was reported that there is strong interaction between polyvinylpyrrolidone (PVP) and hydrophobic carbon materials.[54] As there might exist PVP residue on the Ag-NPs during the synthesis process, is it possible that the interaction between the remnant PVP on the Ag-NPs and pristine-graphene lead to the attachment of Ag-NPs on the pristine-graphene? For this purpose, we prepared bare Ag-NPs without any PVP on their surface via the reduction of $AgNO_3$ by $NaBH_4$ in water without PVP or any other surfactants, and then

© 2013 WILEY-VCH Verlag GmbH & Co. KGaA, Weinheim

did similar mixing process with pristine-graphene. The result shows that the Ag-NPs without any PVP can also be spontaneously attached on pristine-graphene (Figure S4, Supporting Information), experimentally verifying that the van der Waals interactions play the key role in the attachment process. But it should also be mentioned that the residual PVP on the Ag-NPs could be helpful for the attachment of Ag-NPs on pristine-graphene. Therefore, the main driving force for the attachment of Ag-NPs on pristine-graphene is van der Waals interactions, while the presence of residual PVP on the Ag-NPs is beneficial to the attachment process. In order to further clarify the mechanism for the attachment of Ag-NPs on pristine-graphene, control experiments were carried out by mixing RGO with Ag-NPs. It was found that Ag-NPs were severely agglomerated rather than uniformly attached on the RGO (Figure S5, Supporting Information). This might be ascribed to the fact that the electrostatic repulsion between RGO and Ag-NPs is larger than van der Waals forces since both Ag-NPs and RGO carry negative surface charge;[22] thus it would be impossible for the spontaneous absorption of Ag-NPs on RGO. We have also found that the solution medium has a large effect on the synthesis of the pristine-graphene/Ag-NPs hybrids. For example, uniform attachment of Ag-NPs on the pristine-graphene cannot be realized in NMP or water (Figure S6, Supporting Information).

To prove that the intrinsic structures of both the pristine-graphene and the Ag-NPs are not affected in the synthesis process of the pristine-graphene/Ag-NPs hybrids, the as-synthesized pristine-graphene/Ag-NPs hybrids were further characterized by X-ray diffraction (XRD), Raman spectroscopy, and XPS. The XRD pattern of the as-prepared pristine-graphene/Ag-NPs hybrids (Figure 2c) exhibits a diffraction peak at 26.6° corresponding to (002) plane with d-spacing of 0.336 nm of the pristine-graphite,[55] confirming the high quality of the pristine-graphene sheets. The peaks at 38.4° and 44.3° are assigned to the (111) and (200) planes of Ag crystals with face-centered cubic structure, which further suggests that the Ag-NPs are successfully attached on the surface of the pristine-graphene sheets. Raman spectroscopy was used to provide more information on the structural properties of the obtained pristine-graphene/Ag-NPs hybrids (Figure 2d). The enhancement in Raman signals of the pristine-graphen/Ag-NPs hybrids compared with that of the pristine-graphene is due to the SERS effect of the Ag-NPs.[35] It can be seen that the defect-induced D band is almost invisible, which is similar to that of the as-prepared pristine-graphene, demonstrating that the attachment of Ag-NPs on the pristine-graphene surface by this method does not introduce any significant defects into the pristine-graphene. Figure 2e shows the XPS spectrum of Ag 3d3/2 and 3d5/2 doublet with the binding energy located at 374.0 eV and 368.1 eV, suggesting that Ag is present in the metallic form. The C1s spectrum of the pristine-graphene/Ag-NPs hybrids (Figure 2f) shows the absence of C–O species at higher binding energy than C–C peak, further confirming the high-quality of the pristine-graphene sheets. Taken together, the structural characteristics of both the pristine-graphene sheets and the Ag-NPs are not affected in the synthetic process of the pristine-graphene/Ag-NPs hybrids, which means that the as-synthesized pristine-graphene/Ag-NPs hybrids may preserve the unique electronic, mechanical, and optical properties of the defect-free pristine-graphene sheets. Furthermore, the attachment of the Ag-NPs on the pristine-graphene sheets is expected to further enhance their electrical, optical, and catalytic properties. Thus, the as-synthesized pristine-graphene/Ag-NPs hybrids may be exciting materials in the future nanotechnology.

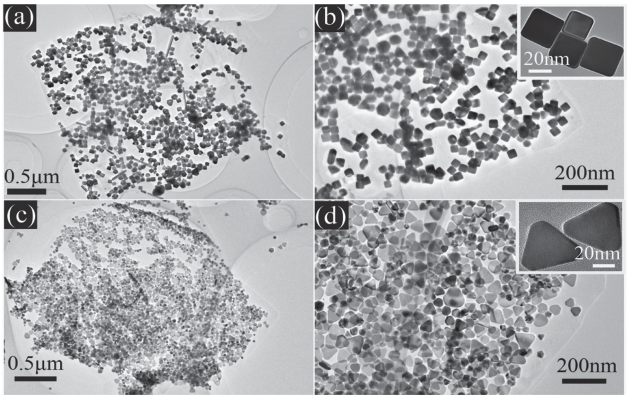

Figure 3. a,b) TEM images of the pristine-graphene/Ag-nanocubes hybrids and c,d) the pristine-graphene/Ag-nanoplates hybrids at different magnifications, respectively.

As metal-NPs show strong shape-dependent properties,[56] control over the morphology of the metal-NPs attached on the pristine-graphene surface is highly desirable. We found that the shape control of metal-NPs attached on the pristine-graphene surface can be easily achieved by selecting metal-NPs with desired-shape in the process of mixing with the pristine-graphene in ethanol. In addition to spherical Ag-NPs (Figure 2a,b), we have also realized homogeneous attachment of Ag-nanocubes (**Figure 3**a,b) and Ag-nanoplates (Figure 3c,d) on the pristine-graphene surface, respectively.

Further experiments demonstrate that not only Ag-NPs but also nanoparticles of other metals with various morphologies can be attached on the pristine-graphene sheets by using our approach. For example, Au-NPs with multi-angular morphology (**Figure 4**a,b) and much smaller nanoparticle-assembled Pd-NPs with a flower-like shape[57] (Figure 4c,d) have been homogeneously attached on the pristine-graphene, as shown in Figure 4.

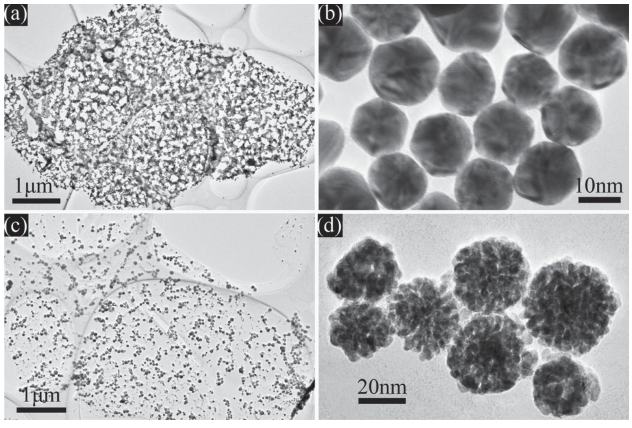

Figure 4. a,b) TEM images of the pristine-graphene/Au-NPs (with multi-angular-shaped morphology) hybrids and c,d) the pristine-graphene/Pd-NPs (with a flower-like shape) hybrids at different magnifications.

© 2013 WILEY-VCH Verlag GmbH & Co. KGaA, Weinheim

Our approach is particularly important since it realized the homogeneous attachment of metal-NPs on the defect-free pristine-graphene surface, which is highly expected but still remains a great challenge up to date. It is especially worth mentioning that this approach allows direct attachment of various metal-NPs with tunable morphologies and packing densities on the pristine-graphene. No additional molecular linkers are needed in the fabrication process, which not only avoids the complicated and tedious surface modification of the pristine graphene or the metal-NPs, but also prevents the disruption of the intrinsic properties of the pristine-graphene by extra functional molecules, and thus facilitates their practical applications. The as-synthesized pristine-graphene/metal-NPs hybrids are expected to combine the shape-tunable optical and electronic properties of the metal-NPs with the unique features of defect-free pristine-graphene, and may have potential applications in SERS, optics, catalysis, and sensors.

One of the most attractive applications of the pristine-graphene/Ag-NPs hybrids is that they may be used as reliable and effective substrates for SERS-based sensors. To estimate the SERS activity of the as-synthesized pristine-graphene/Ag-NPs hybrids (Ag-NPs are in spherical shape as shown in Figure 2a), rhodamine 6G (R6G) was chosen as the probe molecule. The SERS spectra of R6G with different concentrations adsorbed on the as-synthesized pristine-graphene/Ag-NPs hybrids are shown in **Figure 5**a. It can be seen that the Raman intensity decreases with the decrease of the R6G concentration. Even when the R6G concentration was down to 10^{-13} M, the Raman characteristic bands of R6G can still be distinctly observed, demonstrating the high sensitivity of the pristine-graphene/Ag-NPs hybrids as SERS substrates. For a control experiment, the SERS spectra of R6G (10^{-8} M) adsorbed on the bare Ag-NPs used in the fabrication of the pristine-graphene/Ag-NPs hybrids was also collected, as shown in Figure 5b. The pristine-graphene/Ag-NPs hybrids show significantly higher SERS signal than that of the bare Ag-NPs. In addition, the lower detection limit of R6G on the bare Ag-NPs was only 10^{-10} M (Figure S7, Supporting Information), being three orders of magnitude higher than that of the pristine-graphene/Ag-NPs hybrids. In order to optimize the performance of the pristine-graphene/Ag-NPs hybrids as SERS substrates, we further investigated the SERS activity of the pristine-graphene/Ag-NPs hybrids with different densities of Ag-NPs, and found that the pristine-graphene/Ag-NPs hybrids with a low density of Ag-NPs (Figure S3a, Supporting Information) shows lower SERS sensitivity than that with a high density of Ag-NPs (Figure S3b, Supporting Information), as shown in Figure S8, Supporting Information. However, when the density of Ag-NPs further increases (Figure S3c, Supporting Information), the SERS sensitivity shows no significant change anymore. To demonstrate the wide applicability of the pristine-graphene/Ag-NPs to sensitive SERS substrates, we further measured the Raman spectra of another organic molecule, *para*-aminothiophenol (*p*-ATP) by using the pristine-graphene/Ag-NPs as SERS substrates (Figure S9, Supporting Information). It is found that the detection limit of *p*-ATP reaches as low as 10^{-14} M, further confirming the high SERS sensitivity of the pristine-graphene/Ag-NPs hybrids. The high SERS performance of the pristine-graphene/Ag-NPs hybrids can be attributed to the combined effects of the huge surface area of the pristine-graphene to adsorb more target molecules[58] and the strong electromagnetic enhancement of the Ag-NPs.[59] These results indicate that the pristine-graphene/Ag-NPs hybrids are promising SERS substrates for the sensitive detection of chemical and biological analytes.

3. Conclusions

We have demonstrated a generic synthetic approach to large-scale pristine-graphene/metal-NPs hybrids with tunable morphologies and packing densities of the metal-NPs, by heterogeneous mixing of the pristine-graphene produced by liquid-phase exfoliation of graphite in NMP with the pre-synthesized metal-NPs in ethanol solution. This approach is simple, cheap, and environmentally friendly, without any surface modification on the pristine-graphene or the metal-NPs. More importantly, the intrinsic structures of the

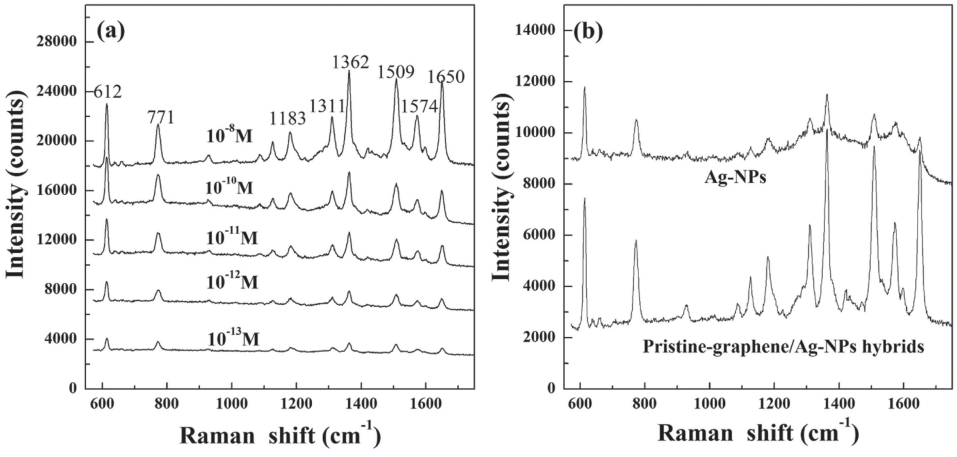

Figure 5. a) SERS spectra of R6G at different concentrations adsorbed on pristine-graphene/Ag-NPs hybrids. b) SERS spectra of 10^{-8} M R6G adsorbed on the pristine-graphene/Ag-NPs hybrids and the bare Ag-NPs, respectively.

© 2013 WILEY-VCH Verlag GmbH & Co. KGaA, Weinheim

pristine-graphene and the metal-NPs are well preserved in the synthetic process of the pristine-graphene/metal-NPs hybrids. The as-synthesized pristine-graphene/Ag-NPs hybrids show very high SERS sensitivity due to the combined effects of large surface area of the pristine-graphene to adsorb more target molecules and the strong electromagnetic enhancement of the Ag-NPs, and may serve as ultrasensitive SERS substrates for the detection of chemical and biological analytes. Our large-scale synthesis of the pristine-graphene/metal-NPs hybrids opens up new opportunities for both fundamental research and potential applications ranging from devices to transparent electrodes and conductive composites. Furthermore, the methodology we used could serve as a generic approach to the development of other pristine-graphene-based hybrids. The ability to realize homogeneous attachment of the shape-controlled metal-NPs on the defect-free pristine-graphene with a scalable, cheap, and environmentally friendly approach may take us a step closer to real-world applications of the pristine-graphene-based hybrids.

4. Experimental Section

Materials: All common reagents and solvents were purchased from the Shanghai Chemical Factory (Shanghai, China) and used as received without further purification. Expandable graphite was purchased from Qingdao Hensen Graphite Co., Ltd. Water used throughout all experiments was purified with the Millipore system.

Preparation of the Pristine-Graphene: To make high quality graphene sheets, we started by first exfoliating commercial expandable-graphite by briefly heating to 950 °C for 20 s in Ar atmosphere. In this process, the intercalating acid was rapidly decomposed and the released energy leads to a sudden and dramatic expansion of the graphite. Then the expanded graphite was dispersed in the NMP at a concentration of 0.1 mg L^{-1} by sonication for 40 min. The resultant dispersion was then centrifuged at 1000 rpm for 10 min. The top half of the graphene dispersion was collected for further use.

Synthesis of the Ag-Nanospheres: Ag-nanospheres were synthesized according to the previous literature with slight modifications.[60] Briefly, 0.05 g PVP ($M_r \approx 55\,000$) were dispersed into 50 mL water by rapid stirring and then heated rapidly to boiling. Then 0.5 mL of 0.1 M $AgNO_3$ and 1 mL of a 1% sodium citrate were added to the above solution in sequence under vigorous stirring, and the resultant solution was held at boiling for 30 min and then cooled in the ambient conditions. Finally, the obtained dispersion was centrifuged and washed five times by ethanol and water, and then dissolved in 20 mL of ethanol.

Synthesis of Ag-Nanocubes: Ag-nanocubes were synthesized according to the reported literature.[61] Briefly, 6 mL ethylene glycol (EG) was heated under stirring for 1 h in a 20 mL glass vial. While the EG was heated, EG solutions containing $AgNO_3$ (48 mg mL^{-1}) and PVP (20 mg mL^{-1}, $M_r \approx 55\,000$) were prepared. A 3 mM solution of NaHS in EG was also prepared 45 min prior to injection. Shortly after injecting 80 µL of the NaHS solution, 1.5 mL and 0.5 mL of the PVP and $AgNO_3$ solutions were sequentially injected, the resultant solution was held at stirring for 10 min, and then cooled in the ambient conditions. Finally, the obtained dispersion was centrifuged and washed five times by ethanol and water, and then dissolved in 20 mL ethanol.

Synthesis of Ag-Nanoplates: Ag-nanoplates were synthesized according to the reported literature.[62] Briefly, 0.2 g PVP ($M_r \approx 55\,000$) was dissolved into 10 mL ethanol, and then 40 mL aniline was added into the above solution under magnetic stirring at room temperature for 20 min. 10 mL of an aqueous solution of 0.2 M $AgNO_3$ was rapidly added into the above solution. The reaction was carried out under magnetic stirring for 30 s, and then kept standing for 24 h at room temperature. Finally, the obtained dispersion was centrifuged and washed five times by ethanol and water, and then dissolved in 20 mL ethanol.

Synthesis of Au-NPs: In a typical synthesis, 0.02 g PVP ($M_r \approx 55\,000$) was dispersed into 20 mL water by rapid stirring and then heated rapidly to boiling. Then 0.5 mL $HAuCl_4$ (0.5 M) and 1 mL sodium citrate (1%) were added to the above solution in sequence under vigorous stirring, and the resultant solution was held at boiling for 30 min then cooled in the ambient conditions. Finally, the obtained dispersion was centrifuged and washed five times by ethanol and water, and then dissolved in 20 mL ethanol.

Synthesis of Pd-NPs: In a typical synthesis, 0.02 g PVP ($M_r \approx 55\,000$) was dispersed into 20 mL water by rapid stirring. Then 1mL H_2PdCl_4 (0.5 M) and 1 mL $NaBH_4$ (0.5%) were added to the above solution in sequence under vigorous stirring. the resultant solution was stirred for 1 h at room temperature. Finally, the obtained stable black dispersion was centrifuged and washed three times with ethanol, and then dissolved in 20 mL ethanol.

Synthesis of the Pristine-Graphene/Metal-NPs Hybrids: In a typical experiment, 1 mL of the pristine-graphene dispersion in NMP was rapidly centrifuged at 15 000 rpm for 10 min. Then the aggregates were mixed with the pre-synthesized metal-NPs in ethanol by brief sonication. The resultant solution was centrifuged at 15 000 rpm for 6 min and then re-suspended in ethanol. This centrifugation and re-suspending process was repeated for three times to ensure complete removal of NMP. Finally, the resultant suspension was held still for several hours, in this process, the metal-NPs will be spontaneously adsorbed onto the pristine-graphene surface to form the pristine-graphene/metal-NPs hybrids.

Structural Characterization of the Pristine-Graphene/Metal-NPs Hybrids: TEM characterization was carried out on a HITACHI H-8100 EM with an accelerating voltage of 200 kV. For TEM observation, carbon-coated copper grids were dipped in the prinstine-graphene/metal-NPs solution and then dried in ambient conditions. XPS measurements were carried out using a VG ESCALAB 220i-XL system, equipped with a monochromatized Al-Ka source ($h\nu$ = 1486.6 eV) for the excitation of photoelectrons. Raman spectra were obtained by using a Renishaw 2000 (Renishaw Co., United Kingdom) equipped with an Ar ion laser giving the excitation line of 514.5 nm with a laser spot diameter of 1.6 µm and air cooling charge-coupled device (CCD) as the detector. The Raman band of a silicon wafer at 520 cm^{-1} was used to calibrate the spectrometer. XRD patterns were recorded using a Bruker D8 Advance X-ray diffractometer with Cu-Ka radiation.

SERS Sensitivity Measurements: To ensure good molecule adsorption, the as-synthesized pristine-graphene/Ag-NPs hybrids spin-coated on Si substrate were immersed in 1 mL R6G aqueous solutions (from 10^{-8} to 10^{-13} M) for 6 h, taken out and then dried in air. All the SERS spectra were acquired with the acquisition time of 5 s.

Supporting Information

Supporting Information is available from the Wiley Online Library or from the author.

Acknowledgements

This work was financially supported by the National Key Basic Research Program of China (Grant 2013CB934304), and the National Natural Science Foundation of China (Grants 61006068, 11274312 and 21201168).

Received: April 25, 2013
Published online: June 20, 2013

© 2013 WILEY-VCH Verlag GmbH & Co. KGaA, Weinheim

[1] K. S. Novoselov, A. K. Geim, S. V. Morozov, D. Jiang, Y. Zhang, S. V. Dubonos, I. V. Grigorieva, A. A. Firsov, *Science* **2004**, *306*, 666.
[2] A. K. Geim, *Science* **2009**, *324*, 1530.
[3] R. R. Nair, P. Blake, A. N. Grigorenko, K. S. Novoselov, T. J. Booth, T. Stauber, N. M. R. Peres, A. K. Geim, *Science* **2008**, *320*, 1308.
[4] C. Lee, X. D. Wei, J. W. Kysar, *Science* **2008**, *321*, 385.
[5] J. Liu, S. Fu, B. Yuan, Y. Li, Z. Deng, *J. Am. Chem. Soc.* **2010**, *132*, 7279.
[6] R. Pasricha, S. Gupta, A. K. Srivastava, *Small* **2009**, *5*, 2253.
[7] Y. C. Si, E. T. Samulski, *Chem. Mater.* **2008**, *20*, 6792.
[8] C. Xu, X. Wang, J. W. Zhu, *J. Phys. Chem. C.* **2008**, *112*, 19841.
[9] S. Yang, X. Feng, L. Wang, K. Tang, J. Maier, K. Mullen, *Angew. Chem. Int. Ed.* **2010**, *49*, 4795.
[10] D. W. Wang, F. Li, J. Zhao, W. Ren, Z.-G. Chen, J. Tan, Z.-S. Wu, I. Gentle, G. Q. Lu, H.-M. Cheng, *ACS Nano* **2009**, *3*, 1745.
[11] D. H. Lee, J. E. Kim, T. H. Han, J. W. Hwang, S. Jeon, S.-Y. Choi, S. H. Hong, W. J. Lee, R. S. Ruo, S. O. Kim, *Adv. Mater.* **2010**, *22*, 1247.
[12] K. E. Byun, D. S. Choi, E. Kim, D. H. Seo, H. Yang, S. Seo, S. H. Hong, *ACS Nano* **2011**, *5*, 8656.
[13] Z. P. Song, T. Xu, M. L. Gordin, Y. B. Jiang, I. T. Bae, Q. F. Xiao, H. Zhan, J. Liu, D. H. Wang, *Nano Lett.* **2012**, *12*, 2205.
[14] D. Wang, D. Choi, J. Li, Z. Yang, Z. Nie, R. Kou, D. Hu, C. Wang, L. V. Saraf, J. Zhang, *ACS Nano* **2009**, *3*, 907.
[15] X. R. Wang, S. M. Tabakman, H. J. Dai, *J. Am. Chem. Soc.* **2008**, *130*, 8152.
[16] U. J. Kim, I. H. Lee, J. J. Bae, S. Lee, G. H. Han, S. J. Chae, F. Günes, J. H. Choi, C. W. Baik, S. Kim, J. M. Kim, Y. H. Lee, *Adv. Mater.* **2011**, *23*, 3809.
[17] S. M. Paek, E. Yoo, I. Honma, *Nano Lett.* **2009**, *9*, 72.
[18] K. Jeon, Z. H. Lee, *Chem. Commun.* **2011**, *47*, 3610.
[19] G. H. Yu, L. B. Hu, M. Vosgueritchian, H. L. Wang, X. Xie, J. R. McDonough, X. Cui, Y. Cui, Z. N. Bao, *Nano Lett.* **2011**, *11*, 2905.
[20] C. X. Peng, B. D. Chen, Y. Qin, S. H. Yang, C. Z. Li, Y. H. Zuo, S. Y. Liu, J. H. Yang, *ACS Nano* **2012**, *6*, 1074.
[21] R. Pasricha, S. Gupta, A. K. Srivastava, *Small* **2009**, *5*, 2253.
[22] W. Ren, Y. X. Fang, E. K. Wang, *ACS Nano* **2011**, *5*, 6425.
[23] K. Jasuja, V. Berry, *ACS Nano* **2009**, *3*, 2358.
[24] R. J. Liu, S. W. Li, X. L. Yu, G. J. Zhang, S. L. Zhang, J. N. Yao, B. Keita, L. Nadjo, L. J. Zhi, *Small* **2012**, *8*, 1398.
[25] A Mastalir, Z. Kiraly, A. Patzko, P. Largentiere, *Carbon* **2008**, *46*, 1631.
[26] G. M. Scheuermann, L. Rumi, P. Steurer, W. Bannwarth, R. Mulhaupt, *J. Am. Chem. Soc.* **2009**, *131*, 8262.
[27] E. Yoo, T. Okata, T. Akita, M. Kohyama, J. Nakamura, I. Honma, *Nano Lett.* **2009**, *9*, 2255.
[28] Y. G. Zhou, J. J. Chen, F. B. Wang, Z. H. Sheng, X. H. Xia, *Chem. Commun.* **2010**, *46*, 5951.
[29] R. S. Sundaram, M. Steiner, H. Y.Chiu, M. Engel, A. A. Bol, R. Krupke, M. Burghard, K. Kern, P. Avouris, *Nano Lett.* **2011**, *11*, 3833.
[30] K. H. Liu, L. Liu, Y. F. Luo, D. M. Jia, *J. Mater. Chem.* **2012**, *22*, 20342.
[31] O. C. Compton, S. T. Nguyen, *Small* **2010**, *6*, 711.
[32] S. J. Park, R. S. Ruoff, *Nat. Nanotechnol.* **2009**, *4*, 217.
[33] X. Q. Fu, F. L. Bei, X. Wang, S. O'Brien, J. R. Lombardi, *Nanoscale* **2010**, *2*, 1461.
[34] Y. Li, X. Fan, J. Qi, J. Ji, S.Wang, G. Zhang, F. Zhang, *Nano Res.* **2010**, *3*, 429.
[35] A. F. Zedan, S. Moussa, J. Terner, G. Atkinson, M. S. El-Shall, *ACS Nano* **2013**, *7*, 627.
[36] Z. Zhang, F. G. Xu, W. S. Yang, M. Y. Guo, X. D. Wang, B. L. Zhang, J. L. Tang, *Chem. Commun.* **2011**, *47*, 6440.
[37] A. N. Sidorova, G. W. Slawinkib, A. H. Jayatissac, F. P. Zamborinib, G. U. Sumanasekerad, *Carbon* **2011**, *50*, 699.
[38] S. Stankovich, D. A. Dikin, R. D. Piner, K. A. Kohlhaas, A. Kleinhammes, Y. Jia, Y. Wu, S. T. Nguyen, R. S. Ruoff, *Carbon* **2007**, *45*, 1558.
[39] G. Eda, G. Fanchini, M. Chhowalla, *Nat. Nanotechnol.* **2008**, *3*, 270.
[40] C. Gomez-Navarro, R. T. Weitz, A. M. Bittner, M. Scolari, A. Mews, M. Burghard, K. Kern, *Nano Lett.* **2007**, *7*, 3499.
[41] W. T. Gu, W. Zhang, X. M. Li, H. W. Zhu, J. Q. Wei, Z. Li, Q. K. Shu, C. Wang, K. L. Wang, W. Shen, F. Y. Kang, D. H. Wua, *J. Mater. Chem.* **2009**, *19*, 3367.
[42] Y. Hernandez, V. Nicolosi, M. Lotya, F. M. Blighe, Z. Sun, S. De, I. T. McGovern, B. Holland, M. Byrne, Y. K. Gun'Ko, J. J. Boland, P. Niraj, G. Duesberg, S. Krishnamurthy, R. Goodhue, J. Hutchison, V. Scardaci, A. C. Ferrari, J. N. Coleman, *Nat. Nanotechnol.* **2008**, *3*, 563.
[43] J. C. Meyer, A. K. Geim, M. I. Katsnelson, K. S. Novoselov, T. J. Booth, S. Roth, *Nature* **2007**, *446*, 60.
[44] A. C. Ferrari, J. C. Meyer, V. Scardaci, C. Casiraghi, M. Lazzeri, F. Mauri, S. Piscanec, D. Jiang, K. S. Novoselov, S. Roth, A. K. Geim, *Phys. Rev. Lett.* **2006**, *97*, 187401.
[45] Z. H. Ni, Y. Y. Wang, T. Yu, Z. X. Shen, *Nano Res.* **2008**, *1*, 273.
[46] J. F. Moulder, W. F. Stickle, P. E. Sobol, K. D. Bomben, *Handbook of X-ray Photoelectron Spectroscopy*, Perkin-Elmer Corporation, Eden Prairie, **1992**.
[47] X. L. Li, G. Y. Zhang, X. D. Bai, X. M. Sun, X. R. Wang, E. Wang, H. J. Dai, *Nat. Nanotechnol.* **2008**, *3*, 538.
[48] T. A. Pham, B. C. Choi, Y. T. Jeong, *Nanotechnology* **2010**, *21*, 465603.
[49] J. B. Liu, S. H. Fu, B. Yuan, Y. L. Li, Z. X. Deng, *J. Am. Chem. Soc.* **2010**, *132*, 7279.
[50] X. M. Geng, L. Niu, Z. Y. Xing, R. S. Song, G. T. Liu, M. T. Sun, G. S. Cheng, H. J. Zhong, Z. H. Liu, Z. J. Zhang, L. F. Sun, H. X. Xu, L. Lu, L. W. Liu, *Adv. Mater.* **2010**, *22*, 638.
[51] J. B. Liu, Y. L. Li, Y. M. Li, J. H. Li, Z. X. Deng, *J. Mater. Chem.* **2010**, *20*, 900.
[52] M. Feng, R. Q. Sun, H. B. Zhan, Y. Chen, *Nanotechnology* **2010**, *21*, 075601.
[53] G. A. Rance, D. H. Marsh, S. J. Bourne, T. J. Reade, A. N. Khlobystov, *ACS Nano* **2010**, *4*, 4920.
[54] M. J. O'Connell, P. Boul, L. M. Ericson, C. Huffman, Y. Wang, E. Haroz, C. Kuper, J. Tour, K. D. Ausman, R. E. Smalley, *Chem. Phys. Lett.* **2001**, *342*, 265.
[55] Z. Q. Li, C. J. Lu, Z. P. Xia, Y. Zhou, Z. Luo, *Carbon* **2007**, *45*, 1686.
[56] A. R. Tao, S. Habas, P. D. Yang, *Small* **2008**, *4*, 310.
[57] A. Mohanty, N. Garg, R. C. Jin, *Angew. Chem. Int. Ed.* **2010**, *49*, 4962.
[58] C. N. R. Rao, A. K. Sood, K. S. Subrahmanyam, A. Govindaraj, *Angew. Chem. Int. Ed.* **2009**, *48*, 7752.
[59] M. Rycenga, C. M. Cobley, J. Zeng, W. Li, C. H. Moran, Q. Zhang, D. Qin, Y. Xia, *Chem. Rev.* **2011**, *111*, 3669.
[60] P. C. Lee, D. Meisel, *J. Phys. Chem.* **1982**, *86*, 3391.
[61] A. R. Siekkinen, J. M. McLellan, J. Y. Chen, Y. N. Xia, *Chem. Phys. Lett.* **2008**, *432*, 491.
[62] J. L. Song, Y. Chu, Y. Liu, L. L Li, W. D Sun, *Chem. Commun.* **2008**, *44*, 1223.

© 2013 WILEY-VCH Verlag GmbH & Co. KGaA, Weinheim